Spectroscopy and spin dynamics for strongly interacting few-spinor bosons in one-dimensional traps

Yanxia Liu,[1] Shu Chen,[2,3,4,*] and Yunbo Zhang[1,†]

[1]*Institute of Theoretical Physics, Shanxi University, Taiyuan 030006, China*

[2]*Beijing National Laboratory for Condensed Matter Physics, Institute of Physics, Chinese Academy of Sciences, Beijing 100190, China*

[3]*School of Physical Sciences, University of Chinese Academy of Sciences, Beijing 100049, China*

[4]*Collaborative Innovation Center of Quantum Matter, Beijing, China*

(Received 12 January 2017; published 20 April 2017)

We consider a one-dimensional trapped gas of strongly interacting few spin-1 atoms which can be described by an effective spin chain Hamiltonian. Away from the SU(3) integrable point, where the energy spectrum is highly degenerate, the rules of ordering and crossing of the energy levels and the symmetry of the eigenstates in the regime of large but finite repulsion have been elucidated. We study the spin-mixing dynamics which is shown to be very sensitive to the ratio between the two channel interactions g_0/g_2 and the effective spin chain transfers the quantum states more perfectly than the Heisenberg bilinear-biquadratic spin chain.

DOI: 10.1103/PhysRevA.95.043628

I. INTRODUCTION

Spinor quantum gases have attracted a lot of attention due to their rich physics in quantum coherence, spin dynamics [1–5], long-range order [6,7], quantum magnetism [8], and symmetry breaking [9]. The majority of research in many-body system has involved trapped spinor atoms such as ^{23}Na and ^{87}Rb experimentally realized in many cold-atom laboratories [10–15]. Among these, spin $s = 1$ system plays a central role in the fundamental understanding of topological quantum phase transition of condensed materials and in modern technologies including, for instance, data storage [16], spin currents [17], spin vortex [6,18], etc. In low-dimensional systems, owing to the liberation of the spin degrees of freedom, a major focus is the understanding of quantum magnetism of higher spin, which have their origin in the underlying microscopic processes between elementary spins.

Recently, the experiment in Heidelberg showed strong evidence that the spin chain of few cold atoms in a one-dimensional system without an underlying lattice can be realized in vicinity of a scattering resonance [19]. On the theoretical side, the general form of the effective spin-chain model for strongly interacting atomic gases with an arbitrary spin in the one-dimensional (1D) traps has been presented [20–26]. This provides a platform for the research of basic magnetic processes in a few-body system. For the two-component system with a large but finite strong s-wave interaction, the transition between the ferromagnetism (FM) and antiferromagnetism (AFM) phases and the theorem on the level crossing between singlet ground state and the maximum spin state have been studied [27–30]. In addition, the effect of a weak additional p-wave interaction on the magnetic orders of the ground state has already been addressed [31,32]. Due to the existence of two-channel interaction, the spin-1 system exhibits much richer phenomena than the two-component system, which is expected to give rise to rich magnetic properties in the strongly interacting limit.

Based on the effective spin-chain model to strongly interacting trapped boson gases with spin 1, we study the properties of the magnetic ground state in the strongly repulsive regime and explore the ordering and crossing of the energy levels when the interaction transfers from the FM to AFM. By analyzing the symmetry of system in the presence of a spin-dependent magnetic gradient and a transverse magnetic field, we show how the ground state may be manipulated and the atoms would collide in the spin-mixing dynamics depending mainly on the ratio between of interaction strengths in the two-collisional channel. Spin-1 systems, in comparison to spin-1/2 systems, offer a better security for encoding and transferring quantum information, primarily due to their larger Hilbert spaces. We further study the quantum state transfer (QST) between the two ends of the spin chain. The effective spin-1 chain provides a site-dependent spin-coupling protocol, due to background trap potential and the resultant inhomogeneous particle density. The effective spin-chain coupling protocol is expected to show more beneficial features than the Heisenberg bilinear-biquadratic (HBB) spin-chain coupling.

The rest of the paper is organized as follows. In Sec. II, we give the detailed spectrum and eigenstates of the effective spin-1 chain model. In Sec. III, based on the effective spin-chain model, we study the spin-changing dynamics and the efficiency and advantage of the QST with this effective spin chain. Finally we conclude in Sec. IV.

II. SPECTROSCOPY

We consider N interacting atoms of hyperfine spin $s = 1$ and mass M in a one-dimensional harmonic trap. The system Hamiltonian is

$$H = \sum_{i=1}^{N} h(x_i) + \sum_{i<j}^{N} (c_0 + c_2 \mathbf{s}_i \cdot \mathbf{s}_j)\delta(x_i - x_j), \qquad (1)$$

where $\mathbf{s}_i = (s_i^x, s_i^y, s_i^z)$ is the spin-1 matrix for the ith atom, $c_0 = (g_0 + 2g_2)/3$ and $c_2 = (g_2 - g_0)/3$ with g_0 and g_2 the coupling constants in the scattering channels with total spin $S = 0$ and 2, respectively [33,34]. For $F = 1$ ^{87}Rb, both the sign and the magnitude of c_2 and hence the magnetic

*schen@iphy.ac.cn

†ybzhang@sxu.edu.cn

nature of the system can be altered significantly in a relatively wide rang by means of a high-resolution photoassociation spectroscopy of the atoms to some excited molecular states as shown in Chapman's experiment [35]. On the other hand, it has been proposed that a multichannel scattering resonance can be achieved for spinor bosons confined in one-dimension geometry with an additional spin-flipping rf field and the interaction in the two channels $S = 0$ and 2 in our system can be tuned to be large simultaneously near the resonance [36]. In the single-particle Hamiltonian

$$h(x) = -\frac{\hbar^2}{2M}\frac{d^2}{dx^2} + \frac{1}{2}M\omega^2 x^2 - Gxs^z + \Omega s^x, \qquad (2)$$

with ω being the trapping frequency, each particle feels a transverse magnetic field of strength Ω and a spin-dependent magnetic gradient of strength G, which are extremely small perturbations and will not cause any noticeable effects in a weakly interacting system [27]. Note that both Ω and G have absorbed in them the Landé factor g_s and the Bohr magneton μ_B. This will change a lot in the strongly interacting system, as can be seen in this study.

Notably, in the absence of the external field, the eigenfunctions of the few-particle system have been exactly solved [21,37,38] by means of the Bose-Fermi mapping in the Tonks-Girardeau limit. The ground-state wave function of a spin-1 system with infinite interaction is described by [21–23]

$$\Psi(x_1,s_1\cdots x_N,s_N) = |\phi_F(x_1\cdots x_N)|\sum_P P[\theta(x_1\cdots x_N)\chi(s_1\cdots s_N)], \qquad (3)$$

where $\theta(x_1\cdots x_N) = 1$ if $x_1 \leqslant \cdots \leqslant x_N$ and zero otherwise, x_i and $s_i = 1,0,-1$ are position and spin indices of the ith particle, respectively. The wave function ϕ_F is taken as the ground state of N spinless fermions, i.e., the Slater determinant made up of the lowest N level of eigenstates, while the spin wave function $|\chi\rangle$ can be written as a superposition of spin Fock states $|m_1 m_2\cdots m_N\rangle$, which means the ith spin is in the m_i state, i.e., $|m_i\rangle = \delta_{s_i m_i}$. The permutation P acts on both the spatial and spin wave functions and ensures the symmetry upon particle exchange. The model in the regime of large but finite repulsion can be mapped to an effective ferromagnetic chain of spin-1 bosons to the first order of g_0^{-1}, g_2^{-1} [22]

$$H_{\text{eff}} = -\sum_{i=1}^{N-1} J_i\left[\frac{1}{g_0}P_0(i,i+1) + \frac{1}{g_2}P_2(i,i+1)\right]. \qquad (4)$$

Instead of representing the model in terms of the permutation operators P_{ij} of neighboring spins [21], we here classify the states according to the collisional channels of total spin S of the two sites. For spin-1 atoms we define the projection operators in the total spin $S = 0$ and $S = 2$ channels as

$$P_0(i,i+1) = \frac{(\mathbf{s}_i\cdot\mathbf{s}_{i+1})^2 - 1}{3} \qquad (5)$$

and

$$P_2(i,i+1) = \frac{(\mathbf{s}_i\cdot\mathbf{s}_{i+1})^2}{6} + \frac{\mathbf{s}_i\cdot\mathbf{s}_{i+1}}{2} + \frac{1}{3} \qquad (6)$$

in the direct sum of the spin space $S = 0 \oplus S = 1 \oplus S = 2$. The effective spin-exchange interaction

$$J_i = 2N!\left(\frac{\hbar^2}{M}\right)^2\int dx_1\cdots dx_N\left|\frac{\partial\phi_F}{\partial x_i}\right|^2 \times\delta(x_i - x_{i+1})\theta(x_1\cdots x_N) \qquad (7)$$

depends on the overlap between the wave functions of neighboring atoms. The structure of the Hamiltonian takes the form of a HBB spin-1 chain [39,40]

$$H = \sum_i[\mathbf{s}_i\cdot\mathbf{s}_{i+1} + \beta(\mathbf{s}_i\cdot\mathbf{s}_{i+1})^2]. \qquad (8)$$

The only difference is that here the coupling constants of neighbor spins are different, due to the background trap potential and the resultant inhomogeneous particle density. The effective spin Hamiltonian H_{eff}, constructed from variational approach and perturbation theory [21–23,25], conserves the square of the total spin operator $\mathbf{S} = \sum_{i=1}^N \mathbf{s}_i$, its z component $S_z = \sum_{i=1}^N s_i^z$, and the parity operator $\Pi = P_{1,N}P_{2,N-1}\ldots$, such that the eigenstates of H_{eff} can be classified in terms of the three quantum numbers: the total spin S, the total magnetization S_z, and the parity Π.

It is intuitive to examine first the eigenvalues and eigenstates of the H_{eff} in the regime of large but finite repulsion $g_0, g_2 \gg 0$. In the simplest case of two particles $N = 2$, we can easily see that the eigenvalues in the channel $S = 2,1,0$ are respectively $-J_1/g_2$, 0, and $-J_1/g_0$. While in the antiferromagnetic spin chain people pay more attention to the degenerate point of singlet and triplet $\beta = -1/3$, which corresponds to Tonks-Girardeau limit $g_0 \to +\infty$ in our case, we focus on the SU(3) integrable point $g_0 = g_2$ where the quintuplet and the singlet have the same energy for the ferromagnetic spin chain. Note that the sign of J, hence the order of the energy levels, is inverted for these two cases, which gives different level crossing point for the ground state. In Fig. 1, we show the energy level dependence on the ratio g_0/g_2, in which each level is $(2S+1)$-fold degenerate in the total spin S channel. We find there exist generally plenty of level crossing in the degenerate point which can be classified into different bunches. To specify them, one needs to denote the eigenstates as $|E_S^n, S_z, \Pi\rangle$, where n labels the bunch of degenerate states occurring at $g_0 = g_2$. The two-particle eigenstates with zero magnetization $S_z = 0$ can be constructed as

$$\left|E_2^1,0,1\right\rangle = (|1,-1\rangle + 2|0,0\rangle + |-1,1\rangle)/\sqrt{6},$$
$$\left|E_0^1,0,1\right\rangle = (|1,-1\rangle - |0,0\rangle + |-1,1\rangle)/\sqrt{3},$$
$$\left|E_1^2,0,-1\right\rangle = (|1,-1\rangle - |-1,1\rangle)/\sqrt{2},$$

on which other states with $S_z = \pm 2, \pm 1$ can be obtained by applying spin raising or lowering operators $S^{\pm}$ repeatedly. We note that two of them belong to the first bunch $n = 1$, while the second bunch $n = 2$ consists of a single level. For the three-particle case with $S_z = 0$, seven levels group into four bunches with the number of levels 2,2,2,1 in each bunch respectively; in the ground-state bunch, the total spin $S = 3$ state with energy $-2J_1/g_2$ competes with the $S = 1$ state with energy $-J_1/2g_2(1/2 + 2\alpha + \sqrt{(2\alpha-1)^2 + 5/4})$, giving rise to the level crossing point at $\alpha = 1$ where $\alpha = (2g_2/g_0 + 1)/3$.

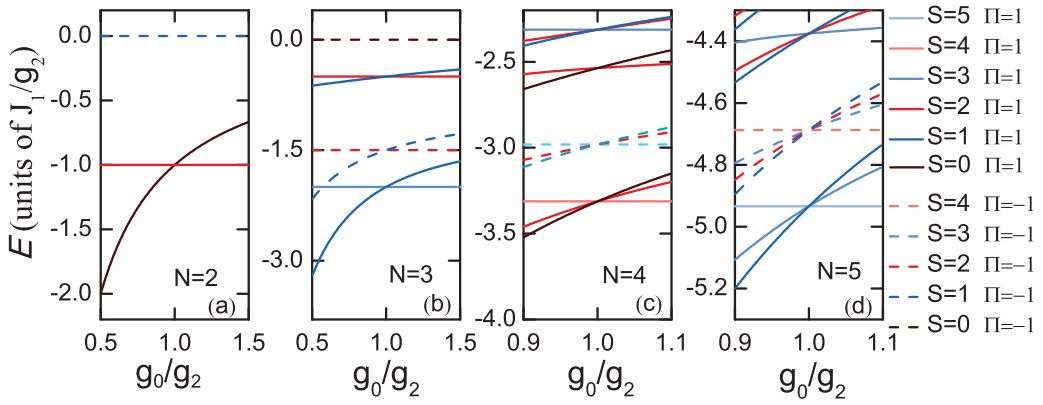

FIG. 1. Energy spectrum of $H_{\rm eff}$ of $N = 2,3,4,5$ particles with total spin S as a function of g_0/g_2. To get a closer look at the law of the energy level crossing, we zoom into the area near $g_0/g_2 = 1$. On the side of $g_0/g_2 < 1$, E^1_S increases with total spin S, and the ground state is a singlet $S = 0$ for $N = 2,4$ and a triplet $S = 1$ for $N = 3,5$ in the lowest bunch. On the side of $g_0/g_2 > 1$, E^1_S increases with decreasing total spin S, and the ground state is FM with $S = N$ in the lowest bunch.

The spectrum of $H_{\rm eff}$ for more particles $N = 4,5$ are shown in Figs. 1(c) and 1(d) by numerically diagonalizing the Hamiltonian (4) in the spin Fock state vector $|m_1 m_2 \ldots m_N\rangle$. It is clearly seen that the spectrum is asymmetric about the integrable point $g_0 = g_2$, at which the ground state is $[(N+1)(N+2)/2]$-fold degenerate. The levels belonging to the same bunch have the same parity: It is always even ($\Pi = 1$) for the ground-state bunch, which contains nevertheless $(N+1)/2$ levels for odd N and $(N+2)/2$ levels for even N, whereas it is always odd ($\Pi = -1$) for the first excited state bunch with $(N-1)$ levels. The total spin in the ground-state bunch are $S = N, N-2, N-4, \ldots$ with step $\Delta S = 2$ and for the first excited state $S = N, N-1, \ldots, 1$ with step $\Delta S = 1$. The two levels with highest total spin $S = N$ and lowest $S = 0(1)$ for even (odd) N are the only two candidates for the ground-state configuration as a consequence of the ferromagnetic or antiferromagnetic coupling of spins. For FM coupling, $g_0/g_2 > 1$, away from the level crossing point, the degenerate energy levels of the bound states are eliminated for different total spin S. For every bunch of degenerate energy levels, the energy decreases with total spin S, i.e., $E^n_{S_1} < E^n_{S_2}$ when $S_1 > S_2$. Therefore, the state with $S = N$ is the ground state with completely symmetric spin wave functions. For AFM coupling $g_0/g_2 < 1$, on the other hand, the energy increases with total spin S, i.e., $E^n_{S_1} < E^n_{S_2}$ when $S_1 < S_2$. Therefore, the states with $S = 1$ (if N is odd) or $S = 0$ (if N is even) have the lowest energy. The emergence of level crossing in the lowest bunch of the energy levels at $g_0 = g_2$ clearly indicates a first-order transition between AFM and FM phases. For N particles, there exist altogether $[N/2]$ independent inhomogeneous spin coupling parameters J_i, with the only result being a slight modification of the energy levels compared with the spectrum without the trapping potential, which nevertheless does not change the ordering and crossing of the levels.

The spectrum of the system is highly degenerate for the total spin S. We now consider the weak spin-dependent magnetic gradient introduced in the single-particle Hamiltonian (2). As schematically shown in Fig. 2, atoms of different spin components are trapped in different potential wells, with the trap center moved to the left or right by an amount $G' = G\hbar/M\omega^2$ depending on the value of spin m. The corresponding effective spin Hamiltonian (4) in the limit of strong interaction will be modified into

$$H'_{\rm eff} = H_{\rm eff} - G\sum_i D_i s_i^z, \tag{9}$$

where $D_i = N!\int x_i |\phi_F|^2 \theta(x_1 \ldots x_N) \prod_{j=1}^N dx_j$ represents the average position of the ith atom. The spin-dependent magnetic

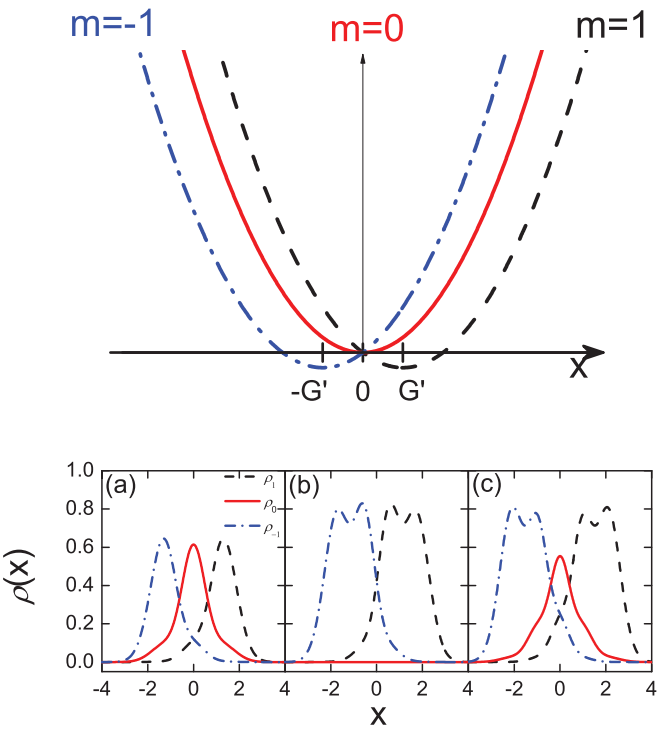

FIG. 2. Potential wells (top) and density distributions (bottom) for $m = -1$ (blue dot-dashed), 0 (red solid), and 1 (black dashed) in subspace $S_z = 0$ for a small value of displacement G' with $G = 2\hbar^2\omega^2/g_2$ and $g_0/g_2 = 1$ obtained from the effective spin model. (a) $N = 3$; (b) $N = 4$; and (c) $N = 5$. The units of the coordinate x and the interaction strength g_2 are $a_{ho} = \sqrt{\hbar/M\omega}$ and $\sqrt{\hbar^3\omega/M}$, respectively.

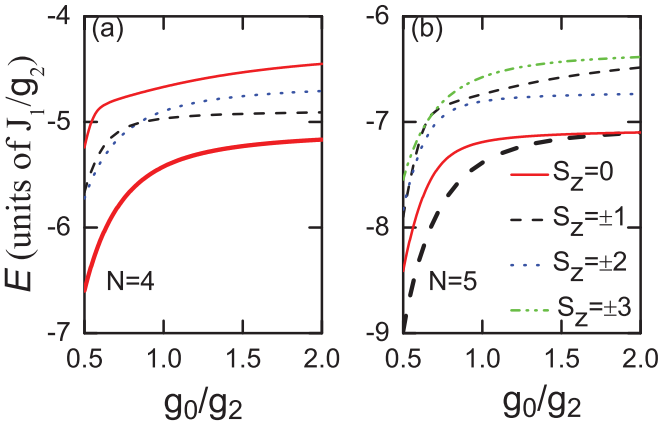

FIG. 3. The lowest few energy levels of $N = 4$ (a) and $N = 5$ (b) classified by S_z as a function of g_0/g_2 for a gradient $G = 2\hbar^2\omega^2/g_2$. Clearly the lowest level for $N = 4$ ($N = 5$) is $S_z = 0$ ($S_z = \pm 1$).

gradient destroys the total spin conservation and parity conservation, implying that $H'_{\rm eff}$ no longer commutes with S^2 and Π. However, we can find that the Hamiltonian $H'_{\rm eff}$ commutes with an operator $T = \Pi \prod_{j=1}^{N} a_j$ [41], where

$$a_j = \begin{pmatrix} 0 & 0 & 1 \\ 0 & 1 & 0 \\ 1 & 0 & 0 \end{pmatrix} \tag{10}$$

serves to flip the spin of jth atom. It is straightforward to show that $\{T, S_z\} = 0$ and $[T, S_z] = 2T S_z$. As a result, T applying to an energy eigenstate $|E_i, S_z\rangle$ changes the state to a degenerate eigenstate $|E_i, -S_z\rangle$, i.e.,

$$T|E_i, S_z\rangle = |E_i, -S_z\rangle. \tag{11}$$

One can also infer from Fig. 3 that adding the magnetic gradient lifts partially the degeneracy of spectrum. The states with total magnetizations S_z and $-S_z$ remain degenerate. The ground state of the system mixes all total spin states to achieve a maximum reduction in energy and thus occurs the spin component separation (bottom of Fig. 2). The first-order transition at $g_0 = g_2$ disappears and the level with total magnetization $S_z = 0$ proves to be the ground state [Fig. 3(a)] for even particle numbers. On the other hand, for odd particle numbers, the state with total magnetization $S_z = \pm 1$ has the lowest energy [Fig. 3(b)].

The density distribution of mth spin component is defined as

$$\rho_m(x) = \sum_i \rho_m^{(i)} \rho^{(i)}(x) \tag{12}$$

with the probability that the magnetization of the ith spin equals m,

$$\rho_m^{(i)} = \sum_{m_1,\ldots,m_N} |\langle m_1, \ldots, m_N|\chi\rangle|^2 \delta_{m,m_i} \tag{13}$$

and the probability to find the ith atom with any spin at position x,

$$\rho^{(i)}(x) = N! \int dx_1 \ldots dx_N \delta(x - x_i)\theta(x_1, \ldots, x_N)|\phi_F|^2. \tag{14}$$

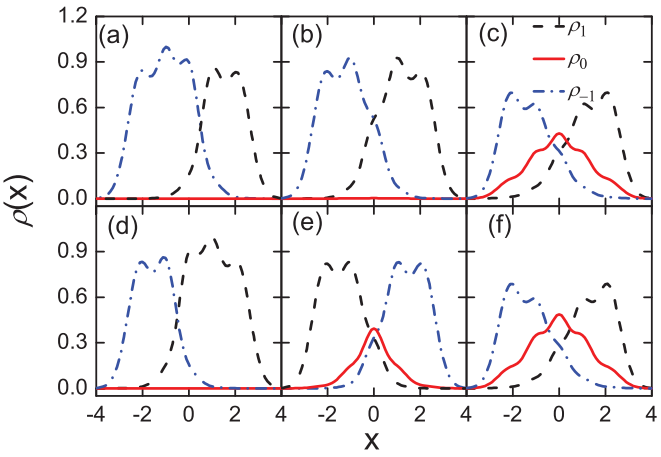

FIG. 4. Effect of transverse magnetic field and nonintegrable interaction on the density distributions of the ground state for spin component 1 (black dashed), 0 (red solid), and -1 (blue dot-dashed) for $N = 5$ and $G = 2\hbar^2\omega^2/g_2$. $g_0/g_2 = 1$ for panels (a)–(d) and $g_0/g_2 = 2$ for panels (e) and (f). Panels (a) and (d) are two degenerate states of $S_z = \pm 1$ with $\Omega = 0$. $\Omega = 0.001\hbar\omega$ for panels (b) and (e) and $\Omega = 0.05\hbar\omega$ for panels (c) and (f).

We show the density distribution for a gradient $G = 2\hbar^2\omega^2/g_2$ in the bottom of Fig. 2. To be more precise, we focus on the SU(3) integrable point $g_0 = g_2$ which guarantees the conservation of atoms in each spin component due to the spin-independent interaction [42]. Surprisingly, we find that the spin-0 component always disappears for even particle numbers in the subspace of the total magnetization $S_z = 0$ [see Fig. 2(b)], while for odd atom numbers the density of spin-0 component remains unity [Figs. 2(a) and 2(c)]. This can be understood by noting that the already fermionized atoms would fill the evenly spaced levels from the bottom one by one, and it is more energetically favorable to put the additional atoms in the left and right traps which are lowered by the gradient by an amount $(G\hbar)^2/2M\omega^2$.

For an applied transverse magnetic field, the effective Hamiltonian $H'_{\rm eff}$, with an additional term ΩS_x included, no longer commutes with S_z and the degeneracy of the system is completely eliminated. However, $H'_{\rm eff}$ still commutes with the operator T. For even atom numbers, the density distributions in the ground state [see, for example, Fig. 2(b)] are hardly modified after the introduction of a very small Ω, which can be regarded as a perturbation to the $S_z = 0$ ground state. For odd atom numbers, the ground state can be constructed as the superposition of two degenerate ground states with $S_z = \pm 1$, whose densities are shown in Figs. 4(a) and 4(d), respectively, i.e.,

$$|G_{\rm odd}\rangle = \frac{1}{\sqrt{2}}(|E_0, S_z = +1\rangle + |E_0, S_z = -1\rangle), \tag{15}$$

with $T|G_{\rm odd}\rangle = |G_{\rm odd}\rangle$. The transverse field plays the role of coupling the two degenerate states such that the ground state is lowered by an amount $\hbar\Omega$. The density profiles of spin $+1$ and spin -1 are now symmetric to each other, due to the conservation of T, implying an combined operation of space inversion and spin flipping, as can be seen in Fig. 4(b). The population in the component spin 0 increases noticeably for a

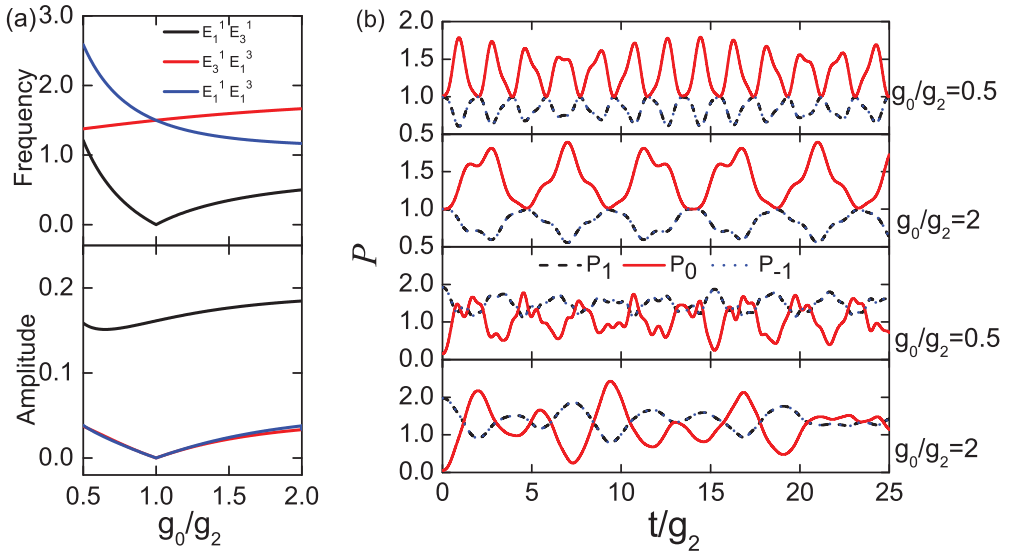

FIG. 5. Frequencies and amplitudes of the population of spin 1 or -1 component vs g_0/g_2 for $N = 3$ (a) and the populations oscillations P_m of spin component $m = 0, \pm 1$ as a function of t/g_2 for $g_0/g_2 = 2$ and $g_0/g_2 = 0.5$. The frequency is in units of $J_1/2\pi\hbar g_2$ and the unit of t/g_2 is $\sqrt{m/\hbar^3\omega^3}$. The top two panels are for $N = 3$ and the bottom two are for $N = 4$. The black dashed curves show the population of $m = 1$, the red solid curves show the population of $m = 0$, and the blue dotted curves show the population of $m = -1$.

strong enough Ω [Fig. 4(c)]. The off-diagonal feature of the S_x matrix would inevitably mix excited states such as that with $S_z = 0$, the spin 0 density of which is significant. An alternative way to introduce the spin-0 component is to bring the system away from the integrable point. We show this in Figs. 4(e) and 4(f) for the case of $g_0/g_2 = 2$, which shows an obvious enhancement of spin-0 density.

III. DYNAMICS

A. Spin-changing dynamics

Realizing spin-chain Hamiltonian with trapped cold atoms offers important applications in the study of microscopic magnetic phenomena. Here we investigate the spin-changing dynamics of this system, which is different from the population dynamics of the weakly interacting system governed by the Gorss-Pitaevskii equation [3,43]. To do this, strongly interacting atoms are initially prepared in the ground state $|\chi(0)\rangle$ with a weak spin-dependent magnetic gradient $G = 2\hbar^2\omega^2/g_2$. The total magnetization S_z is still the conserved quantity, so the system will evolve within one of the S_z subspace. Then the gradient G is abruptly switched off and the evolution of the system is governed by the effective spin chain Hamiltonian $H_{\rm eff}$ in (4). The initial state is realized by obtaining the ground state of Hamiltonian $H'_{\rm eff}$ with nonvanishing G. Starting from the initial state $|\chi(0)\rangle$, the time evolution of the wave function is governed by

$$|\chi(t)\rangle = e^{-\frac{i}{\hbar}H_{\rm eff}t}|\chi(0)\rangle = \sum_i c_i e^{-\frac{i}{\hbar}E_i t}|\phi_i\rangle,$$

where $c_i = \langle\phi_i|\chi(0)\rangle$ is the overlap of the initial state and the ith eigenstate of the system ϕ_i with eigenenergy E_i. We introduce the spin population $P_m(t) = \sum_i \rho_m^{(i)}(t)$ with $\rho_m^{(i)}(t)$ defined in (13) with the replacement $\chi(0) \to \chi(t)$, which measures the population of mth component in the system. For spin-1 system, two atoms in the states -1 and $+1$ have a chance to coherently and reversibly scatter into final states containing two atoms in the state 0, which leads to the population transferring from $P_1(t) + P_{-1}(t)$ to $2P_0(t)$, or vice versa, subject to the conservation of the total population $\sum_m P_m(t) = N$. The system satisfies $P_1(t) - P_{-1}(t) = S_z$ at any time. In this section, we only consider the dynamics in the subspace of total magnetization $S_z = 0$, in which case one must have $P_{+1} = P_{-1}$. We illustrate the spin population dynamics in Fig. 5 for both $P_{\pm1}$ and P_0. In the case of $N = 3$, the initial spin populations for both interaction parameters $g_0/g_2 = 0.5$ and 2 are very close to the case of equally distributed among the three components in the integrable point $g_0 = g_2$. Starting from such an initial population, Rabi-like oscillations of spin populations between the components 0 and ±1 are observed and depicted in Fig. 5(b), which is in sharp contrast to the respectively conservation of atoms in each spin component for $g_0 = g_2$. In the entire range of interaction of interest, we managed to extract the amplitude and the frequency of the oscillation [Fig. 5(a)], and it turns out that the oscillation amplitudes of populations are determined by the weight coefficients of the basis vectors and the oscillation frequencies of populations are determined by the energy differences, among which three energy levels E_1^1, E_3^1, and E_3^3 play dominant roles in the dynamics of the spin-changing collisions. At the integrable point, we find either the frequency or the amplitude of the partial wave would vanish, which ensures the populations in each component remain constant, $P_0(t) = P_{\pm1}(t) = 1$ for $N = 3$ and $P_0(t) = 0$, $P_{\pm}(t) = 2$ for $N = 4$. The intrinsic origin of this exotic phenomenon lies in that this point is highly degenerate. Away from this point, the oscillation frequency of the primary amplitude increases significantly on both sides of $g_0 = g_2$; however, a lower frequency will slow down the oscillation for $g_0/g_2 = 2$. More energy levels are involved in the dynamics of $N = 4$ atoms, the initial spin population

of which is close to the case of equally distributed on the ± 1 components at $g_0 = g_2$. The characteristic dynamics here may be used to detect the quantum phases of the spin-1 chain model, and moreover, may reveal the interesting spin population transfer across the phase boundary by the oscillation frequency.

B. Quantum state transfer

Spin chains have important applications in quantum simulation and computation. The spin chains have been proposed intensively as quantum channels to study state transfer in small quantum networks [44–46]. Perfect quantum-state transfer is very important to accomplish prospective quantum information processing through a chain of nearest-neighbor coupled spins. The interaction energy of each qutrit-qutrit pair in the translation-invariant HBB spin-1 chain is the same, which can be described by the Hamiltonian (8) with $\beta = (2g_2/g_0 + 1)/3$, but in our effective spin chain this interaction energy (7) is site dependent. Here, we study the superiority of the inhomogeneous effective spin-1 chain as a quantum channel.

Transferring a known or unknown quantum state with spin-1 from one place to another has been studied in Refs. [47,48]. In the original proposal, the quantum-state transfer protocol involves initializing the spin chain of N sites with the first spin in an arbitrary state $|\psi\rangle = \xi_{-1}|-1\rangle + \xi_0|0\rangle + \xi_1|1\rangle$ ($\sum_m |\xi_m|^2 = 1$) and decoupled from the rest of the chain. At $t = 0$, the first and second spins abruptly couple and let the system freely evolve in the spin chain. At time t, the quality of the transfer of $|\psi\rangle$ to the last spin of the chain is evaluated by the fidelity of attaining $|\psi\rangle$ at site N. Ideal transfer would imply that at time t^* the last spin of the chain is in state $|\psi\rangle$. We consider a simple case, at time $t = 0$ its state was $|\Psi(0)\rangle = |-1,1\ldots 1\rangle$. Our aim is to maximize the probability of retrieving state $|1\ldots 1,-1\rangle$ at time t^*. We define the fidelity of state transfer as

$$F(t) \equiv |\langle\Psi(t)|1\ldots 1,-1\rangle|^2,$$

which relies only on the expansion coefficients of the eigenstates $|E_S^n\rangle$ expanded in the basis vectors $|1\ldots 1,-1\rangle$ and $|-1,1\ldots 1\rangle$. Let $F \equiv F(t^*)$ be the maximum value that achieves in the intermediate time. We plot the maximum of fidelity F of the state transfer in Fig. 6 as a function of g_0/g_2. For a system of $N = 4$ with the trap frequency $\omega = 40\,\mathrm{kHz}$ and the interaction strength $g_2 = 20$ in units of $\sqrt{\hbar^3\omega/M}$, the occurrence time of the maximal fidelity t^* ranges from 10^{-2} to 1.5 s, which appears, however, randomly for varying g_0/g_2. We compare the fidelity F of the HBB and effective spin chains of length $N = 4$ to 8 in Fig. 6, which reflects that the effective spin chain transfers the state more faithfully than the HBB spin chain, especially for longer spin chain. With the increase of particle number N, the overall trend is that F decreases. At the integrable point $g_0/g_2 = 1$, F reaches a maximum value in the both spin chain models, while the effective spin chain model always provides more efficient way for quantum state transfer in the entire interaction regime.

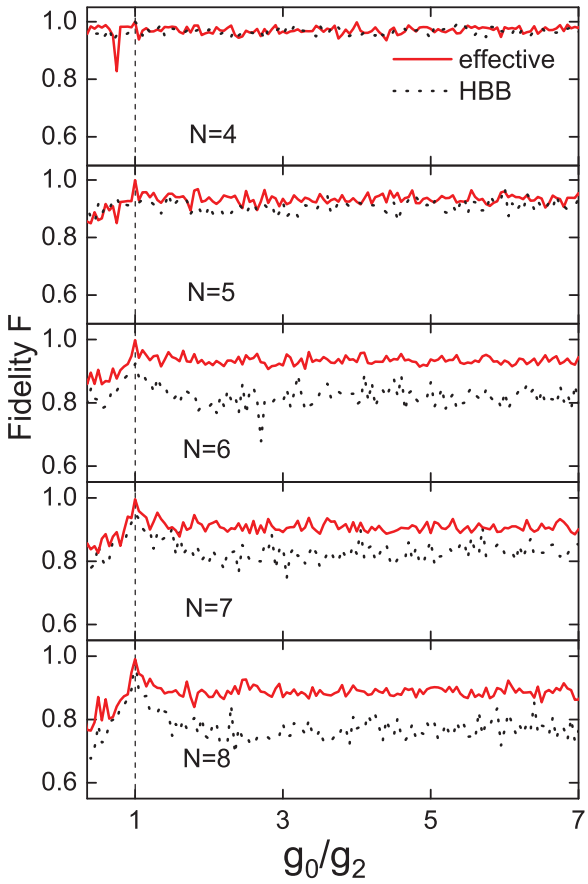

FIG. 6. Maximum value of the fidelity F of state transfer in a spin-1 system with particle numbers $N = 4$ to 8, for the HBB spin chain (black dotted) and the effective spin chain (red solid). Vertical dotted line indicates the phase transition point $g_0/g_2 = 1$.

IV. CONCLUSIONS

We have shown that a three-component system of strongly interacting bosonic atoms in a one-dimensional (1D) harmonic trap can be represented effectively as a spin chain described by the bilinear-biquadratic spin-1 model Hamiltonian. For few atoms in the trap, we have determined the energy spectrum of the ground states and obtained the rules of the ordering and crossing of energy levels near the first-order quantum phase transition, i.e., the SU(3) integrable point, $g_0 = g_2$. The energy levels of the eigenstates are collected into different bunches which can be labeled by the total spin and the parity. Away from the degenerate point, the ground state is either with highest total spin $S = N$ for FM coupling between atoms, or with lowest spin $S = 1$ (for odd N) or $S = 0$ (for even N) for AFM coupling $g_0/g_2 < 1$. We further introduce a magnetic gradient to remove the degeneracy on S, motivated by the experimental studies of coherent multiflavor spin dynamics in a fermionic quantum gas [49], and subsequently study the quench dynamics of the ground states of spin-component separation when the initial magnetic gradient is removed quickly. Our results reveal the spin-change dynamics of the system governed by the ratio of interactions between the two channels. Through the study of the dynamics of the quantum

state transfer, we show that the inhomogeneous qutrit-qutrit interaction of the engineered effective spin chain is more efficient in state transferring.

Note added. Recently, we became aware of two papers on spin dynamics in strongly interacting systems in the case of two-component Fermi and Bose systems that have been published in [50,51], where the quantum state transfer in different settings are discussed.

ACKNOWLEDGMENTS

Y.Z. would like thank Han Pu for helpful discussion. This work is supported by NSF of China under Grants No. 11474189, No. 11674201, and No. 11234008, Program for Changjiang Scholars, and Innovative Research Team in University (PCSIRT) (No. IRT13076). S.C. is supported by NSF of China under Grants No. 11425419, No. 11374354, and No. 11174360.

[1] D. M. Stamper-Kurn and M. Ueda, Rev. Mod. Phys. **85**, 1191 (2013).
[2] C. K. Law, H. Pu, and N. P. Bigelow, Phys. Rev. Lett. **81**, 5257 (1998).
[3] M.-S. Chang, C. D. Hamley, M. D. Barrett, J. A. Sauer, K. M. Fortier, W. Zhang, L. You, and M. S. Chapman, Phys. Rev. Lett. **92**, 140403 (2004).
[4] B. Naylor, M. Brewczyk, M. Gajda, O. Gorceix, E. Maréchal, L. Vernac, and B. Laburthe-Tolra, Phys. Rev. Lett. **117**, 185302 (2016).
[5] W. Zhang, S. Yi, and L. You, New J. Phys. **5**, 77 (2003).
[6] S. Yi and H. Pu, Phys. Rev. Lett. **97**, 020401 (2006).
[7] L. Santos and T. Pfau, Phys. Rev. Lett. **96**, 190404 (2006).
[8] D. L. Campbell, R. M. Price, A. Putra, A. Valdés-Curiel, D. Trypogeorgos, and I. B. Spielman, Nat. Commun. **7**, 10897 (2016).
[9] N. Navon, A. L. Gaunt, R. P. Smith, and Z. Hadzibabic, Science **347**, 167 (2015).
[10] D. M. Stamper-Kurn, M. R. Andrews, A. P. Chikkatur, S. Inouye, H.-J. Miesner, J. Stenger, and W. Ketterle, Phys. Rev. Lett. **80**, 2027 (1998).
[11] Y. Liu, E. Gomez, S. E. Maxwell, L. D. Turner, E. Tiesinga, and P. D. Lett, Phys. Rev. Lett. **102**, 225301 (2009).
[12] M. Vengalattore, S. R. Leslie, J. Guzman, and D. M. Stamper-Kurn, Phys. Rev. Lett. **100**, 170403 (2008).
[13] D. Jacob, L. Shao, V. Corre, T. Zibold, L. De Sarlo, E. Mimoun, J. Dalibard, and F. Gerbier, Phys. Rev. A **86**, 061601(R) (2012).
[14] A. Vinit, E. M. Bookjans, C. A. R. Sa de Melo, and C. Raman, Phys. Rev. Lett. **110**, 165301 (2013).
[15] T. Fukuhara, A. Kantian, M. Endres, M. Cheneau *et al.*, Nat. Phys. **9**, 235 (2013).
[16] V. S. Morozov, Z. B. Etienne, M. C. Kandes, A. D. Krisch, M. A. Leonova, D. W. Sivers, V. K. Wong, K. Yonehara, V. A. Anferov, H. O. Meyer, P. Schwandt, E. J. Stephenson, and B. von Przewoski, Phys. Rev. Lett. **91**, 214801 (2003).
[17] J. Sinova, D. Culcer, Q. Niu, N. A. Sinitsyn, T. Jungwirth, and A. H. MacDonald, Phys. Rev. Lett. **92**, 126603 (2004).
[18] T. Li, S. Yi, and Y. Zhang, Phys. Rev. A **92**, 063603 (2015); **93**, 053602 (2016).
[19] S. Murmann, F. Deuretzbacher, G. Zürn, J. Bjerlin, S. M. Reimann, L. Santos, T. Lompe, and S. Jochim, Phys. Rev. Lett. **115**, 215301 (2015).
[20] F. Deuretzbacher, K. Fredenhagen, D. Becker, K. Bongs, K. Sengstock, and D. Pfannkuche, Phys. Rev. Lett. **100**, 160405 (2008).
[21] F. Deuretzbacher, D. Becker, J. Bjerlin, S. M. Reimann, and L. Santos, Phys. Rev. A **90**, 013611 (2014).
[22] L. Yang and X. Cui, Phys. Rev. A **93**, 013617 (2016).
[23] L. Yang, L. Guan, and H. Pu, Phys. Rev. A **91**, 043634 (2015).
[24] L. Yang and H. Pu, Phys. Rev. A **94**, 033614 (2016).
[25] E. J. Lindgren, J. Rotureau, C. Forssen, A. G. Volosniev, and N. T. Zinner, New J. Phys. **16**, 063003 (2014).
[26] A. G. Volosniev, D. Petrosyan, M. Valiente, D. V. Fedorov, A. S. Jensen, and N. T. Zinner, Phys. Rev. A **91**, 023620 (2015).
[27] X. Cui and T.-L. Ho, Phys. Rev. A **89**, 023611 (2014).
[28] E. H. Lieb and D. Mattis, Phys. Rev. **125**, 164 (1962).
[29] L. Guan and S. Chen, Phys. Rev. Lett. **105**, 175301 (2010); L. Guan, S. Chen, Y. Wang, and Z. Q. Ma, *ibid.* **102**, 160402 (2009).
[30] H. Hu, L. Guan, and S. Chen, New J. Phys. **18**, 025009 (2016).
[31] L. Yang, X. Guan, and X. Cui, Phys. Rev. A **93**, 051605 (2016).
[32] H. Hu, L. Pan, and S. Chen, Phys. Rev. A **93**, 033636 (2016).
[33] T.-L. Ho, Phys. Rev. Lett. **81**, 742 (1998).
[34] T. Ohmi and K. Machida, J. Phys. Soc. Jpn. **67**, 1822 (1998).
[35] C. D. Hamley, E. M. Bookjans, G. Behin-Aein, P. Ahmadi, and M. S. Chapman, Phys. Rev. A **79**, 023401 (2009).
[36] X. Cui, Phys. Rev. A **90**, 022705 (2014).
[37] M. D. Girardeau, J. Math. Phys. **1**, 516 (1960).
[38] M. D. Girardeau, Phys. Rev. A **82**, 011607(R) (2010).
[39] I. Affleck, J. Phys.: Condens. Matter **1**, 3047 (1989).
[40] S. K. Yip, Phys. Rev. Lett. **90**, 250402 (2003).
[41] L. Chen, H. Pu, and Y. Zhang, Phys. Rev. A **93**, 013629 (2016).
[42] Y. Jiang, P. He, and X.-W. Guan, J. Phys. A **49**, 174005 (2016).
[43] J. Kronjäger, C. Becker, P. Navez, K. Bongs, and K. Sengstock, Phys. Rev. Lett. **97**, 110404 (2006).
[44] S. Bose, Phys. Rev. Lett. **91**, 207901 (2003).
[45] S. Bose, Contemp. Phys. **48**, 13 (2007).
[46] D. Burgarth, Eur. Phys. J. Special Topics **151**, 147 (2007).
[47] J. Ghosh, Phys. Rev. A **90**, 062318 (2014).
[48] M. Wieśniak, A. Dutta, and J. Ryu, Acta Phys. Pol. A **128**, 3 (2015).
[49] J. S. Krauser, J. Heinze, N. Fläschner, S. Götze, O. Jürgensen, D. S. Lühmann, C. Becker, and K. Sengstock, Nat. Phys. **8**, 813 (2012).
[50] O. V. Marchukov, E. H. Eriksen, J. M. Midtgaard, A. A. S. Kalaee, D. V. Fedorov, A. S. Jensen, and N. T. Zinner, Eur. Phys. J. D **70**, 32 (2016).
[51] N. J. S. Loft, O. V. Marchukov, D. Petrosyan, and N. T. Zinner, New J. Phys. **18**, 045011 (2016).